Title
TRIAXIAL SHAPES IN LIGHT La NUCLEI

Authors
Butler, P.A.
Meyer-ter-Vehn, J.
Ward, D.
et al.

Publication Date
1975-03-01

Submitted to Physics Letters B

LBL-3483 c.1
Preprint

TRIAXIAL SHAPES IN LIGHT La NUCLEI

P. A. Butler, J. Meyer-ter-Vehn, D. Ward, H. Bertschat,
P. Colombani, R. M. Diamond, and F. S. Stephens

March 1975

Prepared for the U. S. Atomic Energy Commission
under Contract W-7405-ENG-48

TRIAXIAL SHAPES IN LIGHT La NUCLEI*

P. A. Butler,[†] J. Meyer-ter-Vehn,[‡] D. Ward,[§] H. Bertschat,[||]
P. Colombani,[¶] R. M. Diamond, and F. S. Stephens

Lawrence Berkeley Laboratory
University of California
Berkeley, California 94720

ABSTRACT

Lifetimes for the lowest $15/2^-$ and $19/2^-$ states in ^{129,131}La have been measured. Values for the reduced transition probabilities compared with those in neighboring even nuclei can be understood using a model that couples a rotation-aligned $h_{11/2}$ proton to a triaxial core.

---

*Work performed under the U. S. Energy Research and Development Administration.

[†] U.K. S.R.C./N.A.T.O. Fellow.

[‡] Permanent address: TU München, 8046 Garching, West Germany.

[§] Permanent address: Chalk River Nuclear Laboratories, Ontario, Canada

[||] D.A.A.D. Fellow; permanent address: Hahn-Meitner-Institut, Berlin, West Germany

[¶] Permanent address: Institut de Physique Nucléaire, 91406 Orsay, France.

A systematic feature of the light lanthanum isotopes is the occurrence of a sequence of yrast levels, $11/2^-$, $15/2^-$, $19/2^-$, etc., whose energy spacings are very similar to the spacings of the levels, 0^+, 2^+, 4^+, etc., of the neighboring doubly-even nuclei [1]. These levels have been identified as a decoupled band in which an $h_{11/2}$ proton has its spin maximally aligned with the rotation axis of a prolate core. A number of such examples have since been observed, but in some cases it has been shown [2] that the data available on additional states indicate deviations from axial symmetry. As a test of the triaxial description we have measured lifetimes for the $15/2^-$ and $19/2^-$ levels in ^{129,131}La.

We have used the recoil-distance method, see, for example, ref. [3], to measure lifetimes using the reactions ^{119}Sn(^{14}N,4n)^{129}La at 67 MeV, ^{118}Sn(^{16}O,4n)^{130}Ce at 82 MeV and ^{116}Cd(^{19}F,4n)^{131}La at 72 MeV. The heavy-ion beams were provided by the LBL 88-inch cyclotron. The Sn targets were stretched self-supporting foils of 0.75 mg cm^{-2} thickness. The Cd target was 0.6 mg cm^{-2} of enriched Cd evaporated on 0.2 mg cm^{-2} nickel. Gamma rays were detected in a planar Ge detector placed at 0^o with respect to the beam direction. For the lowest transitions in the yrast sequence, recoil-distance decay curves were derived by integrating the stopped (I_s) and moving (I_m) γ-ray peaks and plotting the ratio $I_s/(I_s+I_m)$ versus plunger setting. In the ^{131}La case (Fig. 1) at the greatest distances used, corresponding to 400 and 1600 psec flight time, a stopped component of 14% was evident in the $15/2^- \rightarrow 11/2^-$ transition. This is mostly due to side feeding directly into the 2^+ state. The ratios plotted in Fig. 1 have been corrected for this component.

The average recoil velocity was derived from the centroid shifts of stopped and moving γ-ray components, and after correction for the finite solid angle of the Ge detector was found to be 0.87% of c for ^{129}La, 1.03% for ^{130}Ce and 1.05% for ^{131}La. In all cases there was an appreciable spread in the projected velocities of the recoils due to target thickness and finite size of the cone of the recoiling ions. But taking this into account explicitely did not yield results differing significantly from those using the average velocity described above.

For each nucleus, lifetimes for the $19/2^-(4^+)$ and $15/2^-(2^+)$ levels were obtained by fitting simultaneously the two decay curves using a least-squares fitting procedure. The behaviour of the feeding ahead of the $19/2^-$ state, approximated by two or more levels whose lifetimes were free parameters, could be determined partly by the shape of the $23/2^- \rightarrow 19/2^-$ decay curve and partly by the constraint that all the curves pass through a common origin. Where the experimental relative intensities of the cascade transitions markedly decreased with increasing spin, feeding into the band from other levels was also taken into account. The results are shown in Table 1, where it can be seen that for ^{130}Ce, the only case where other measurements are available for comparison, the present value for the $2 \rightarrow 0$ transition is in excellent agreement with that measured by Dehnhardt et al. [4].

Calculated B(E2) values for transitions between the lowest yrast states of an $h_{11/2}$-quasiparticle coupled to an asymmetric core are shown in Fig. 2. A difference in this triaxial case from the more usual axially symmetric calculation is that for the $11/2^-$, $15/2^-$ and $19/2^-$ states the total angular momentum tends to localize about the intrinsic $\hat{2}$-axis instead of precessing in the $(\hat{1},\hat{2})$-plane. (We are using a system of axes where the $\hat{2}$-axis is the oblate symmetry axis at $\gamma = 60^{\circ}$ and the $\hat{3}$-axis is the prolate symmetry axis at $\gamma = 0^{\circ}$). The $\hat{2}$-axis is preferred because this maximizes the overlap between the core and the particle. The transitions between the lowest yrast states therefore occur with the total angular momentum pointing along the $\hat{2}$-axis. In this case, the E2-transition probability can be approximated by

$$B(E2)_{\text{class}} \cong \frac{5}{16\pi} \left(Q_{22}^{(\hat{2})}\right)^2$$

where $Q_{22}^{(\hat{2})} = Q_0 \cdot \sin(\gamma - 60^{\circ}) / \sqrt{2}$ is the $\mu = 2$ component of the intrinsic quadrupole tensor related to the $\hat{2}$-axis (lower dashed line in Fig. 2). As $\gamma \rightarrow 60^{\circ}$, $B(E2)_{\text{class}}$ decreases since the nuclear shape becomes increasingly symmetric about the $\hat{2}$-axis and $Q_{22}^{(\hat{2})} \rightarrow 0$. The exactly calculated B(E2)'s for the $15/2^{-} \rightarrow 11/2^{-}$ and the $19/2^{-} \rightarrow 15/2^{-}$ transitions closely follow this classical limit over the range $10^{\circ} < \gamma < 35^{\circ}$ (Fig. 2). Beyond $\gamma = 35^{\circ}$, the rotation-aligned 15/2 state crosses the 15/2 state of the 11/2[505] Nilsson band which is lower in energy near $\gamma = 60^{\circ}$. This explains the oscillations of $B(E2;\, 15/2^{-} \rightarrow 11/2^{-})$ and $B(E2;\, 19/2^{-} \rightarrow 15/2^{-})$ between $35^{\circ} < \gamma < 45^{\circ}$. For states with $I > 19/2$ the total angular momentum of the system tends to align with the $\hat{1}$-axis, since this axis has the largest moment of inertia in the triaxial region, and thereby minimizes the core rotational energy. This tendency now dominates over the preference of the particle for the $\hat{2}$-axis. The B(E2)'s of higher transitions (e.g. $27/2^{-} \rightarrow 23/2^{-}$) therefore peak near $\gamma = 30^{\circ}$ where $Q_{22}^{(\hat{1})} = Q_0 \cdot \sin(\gamma + 60^{\circ}) / \sqrt{2}$ has its maximum (upper dashed line in Fig. 2).

The B(E2) values calculated from the asymmetric rotor model with $\gamma = 22°$ (^{129}La) and $\gamma = 23°$ (^{131}La) are also shown in Table 1 together with predictions of the symmetric rotor model and the weak coupling model. The values of γ are obtained from the energy ratios of the 2^+, $2^{+'}$, and 4^+ levels in ^{130}Ba and the systematics in the heavier Ba nuclei [2]. The experimental results for the $15/2^- \rightarrow 11/2^-$ and $19/2^- \rightarrow 15/2^-$ transitions in ^{129}La and ^{131}La, plotted also in Fig. 2, are seen to follow closely the predictions of the asymmetric model. The predictions of weak coupling for the B(E2; $15/2^- \rightarrow 11/2^-$) values are next best, but they differ significantly from the experimental results, being systematically smaller in magnitude. The lack of precise experimental data on the core $4^+ \rightarrow 2^+$ transition makes further quantitative comparison with the weak coupling model difficult, but with the additional assumption of a simple rotational or vibrational core one would obtain a value of respectively 1.4 and 2.0 for the ratio B(E2; $19/2^- \rightarrow 15/2^-$): B(E2; $15/2^- \rightarrow 11/2^-$) in contradiction to the experimental evidence.

The recent result by Häusser et al. [5] in ^{107}Cd can be shown to follow a similar trend as the La data. Their experimental value for B(E2; $15/2^- \rightarrow 11/2^-$) : B(E2; $2^+ \rightarrow 0^+$) of 1.16 ± 0.11 is in agreement with the triaxial result 1.17 calculated using the value of $\gamma = 22°$ obtained from ^{106}Cd. The experimental result significantly differs from the value of 1.46 calculated using $\gamma = 0°$. It should be noted that the results shown in Fig. 2 are rather independent of the two other model parameters $\beta \cdot A^{2/3}$ and λ_F. Calculated B(E2) values differ by less than the experimental errors when changing these parameters between their values for ^{107}Cd and ^{129,131}La.

In conclusion, we have found that the model of a particle coupled to a triaxial rotor gives a quantitative interpretation of the B(E2; $15/2^- \rightarrow 11/2^-$) values in ^{107}Cd and ^{129,131}La and also of the B(E2; $19/2^- \rightarrow 15/2^-$) values in ^{129,131}La. Important information regarding the triaxial-rotor model also comes from the energies of the other unique-parity levels seen in these nuclei. In particular, the energies of the unfavoured states ($j + 1$, $j + 3$, $j + 5$, ...) depend rather sensitively on the shape asymmetry and strongly indicate triaxial shapes both in the La region and in the Ir - Tℓ region. It thus appears that this model gives a simple and intuitive explanation for all the features so far observed for these unique-parity orbitals.

REFERENCES

1. J. R. Leigh, K. Nakai, K. H. Maier, F. Pühlhofer, F. S. Stephens and R. M. Diamond, Nucl. Phys. A213 (1973) 1; F. S. Stephens, R. M. Diamond, J. R. Leigh, T. Kammuri and K. Nakai, Phys. Rev. Lett. 29 (1972) 438.
2. J. Meyer-ter-Vehn, F. S. Stephens, and R. M. Diamond, Phys. Rev. Lett. 32 (1974) 1383;

   J. Meyer-ter-vehn, submitted to Nuclear Physics.
3. D. B. Fossan and E. K. Warburton, "Nuclear Spectroscopy and Reactions" (Ed. J. Cerny, Academic Press 1974) Part C, p. 307.
4. W. Dehnhardt, S. J. Mills, M. Müller-Veggian, U. Neumann, D. Pelte, G. Poggi, B. Povh and P. Taras, Nucl. Phys. A225 (1974) 1.
5. O. Häusser, D. J. Donahue, R. L. Hershberger, R. Lutter, F. Riess, H. Bohn, T. Faestermann, F. v. Feilitzsch and K. E. G. Löbner, Phys. Lett. 52B (1974) 329.
6. W. Kutschera, W. Dehnhardt, O. C. Kistner, P. Kump, B. Povh and H. J. Sann, Phys. Rev. C5 (1972) 1658.
7. C. W. Towsley, R. Cook, D. Cline and R. N. Horoshko, J. Phys. Soc. Japan 34, Suppl. (1973) 442.

Table 1. Lifetimes and B(E2) values in ^{129,131}La, ^{107}Cd, and their respective core nuclei. The experimental results are compared with predictions from various theoretical models.

Nucleus	E_γ (keV)	τ (psec)	B(E2)↓exp. (e^2b^2)	Theory				
				Strong coupling		Weak coupling	Rotation aligned (triaxial core)	
				K = 1/2	K = 11/2		γ = 0	γ_{exp}*
^{128}Ba								
2→0	279	140 ± 30 [6]	0.33 ± 0.07					
^{130}Ce								
2→0	254	225 ± 19 [4] 211 ± 9 a)	0.33 ± 0.02					
^{129}La								γ = 22°
15/2→11/2	269	130 ± 6 a)	0.42 ± 0.02	0.53	0.07	0.33	0.50	0.37 †
19/2→15/2	475	8.7 ± 1.3 a)	0.38 ± 0.06	0.55	0.22		0.52	0.42 †
^{130}Ba								
2→0	357		0.24 ± 0.08 [7]					
^{132}Ce								
2→0	325	67.9 ± 9.5 [4]	0.32 ± 0.05					
^{131}La								γ = 23°
15/2→11/2	336	55 ± 2 a)	0.34 ± 0.02	0.49	0.06	0.30	0.45	0.32 ††
19/2→15/2	533	5.8 ± 0.6 a)	0.33 ± 0.03	0.50	0.20		0.47	0.37 ††
^{106,108}Cd								
2→0	633		0.082 ± 0.006 [5]					γ = 22°
^{107}Cd								
15/2→11/2	515	23.5 ± 1.5 [5]	0.095 ± 0.006	0.132	0.02	0.082	0.12	0.096†††

Footnotes to Table 1

---

[a] Present results.

[*] Estimated from the systematics of the 2^+, $2^{+\prime}$, and 4^+ levels in the core nuclei.

[†] Model parameters: $\beta \cdot A^{2/3} = 6.8$ derived from B(E2; $2^+ \rightarrow 0^+$) of core nuclei, Fermi energy $\lambda_F = (\varepsilon_1 + \varepsilon_2)/2$ estimated from Nilsson level scheme (ε_ν s.p. energies of $h_{11/2}$ shell), $\Delta = 1.0$ MeV from odd-even mass differences.

[††] Model parameters: $\beta \cdot A^{2/3} = 6.4$, $\lambda_F = (\varepsilon_1 + \varepsilon_2)/2$, $\Delta = 1.0$ MeV derived in the same way as for ^{129}La.

[†††] Model parameters: $\beta \cdot A^{2/3} = 4.0$, $\lambda_F = \varepsilon_1$, $\Delta = 1.3$ MeV derived in the same way as for ^{129}La.

FIGURE CAPTIONS

Fig. 1. Recoil-distance decay curve for ^{131}La.

Fig. 2. Calculated transition probabilities as functions of the core asymmetry γ. The calculations are accurate to within about 5% for a range of $\beta \cdot A^{2/3}$ given by $4 \leq \beta \cdot A^{2/3} \leq 7$ and a range of λ_F given by $\varepsilon_1 \leq \lambda_F \leq \varepsilon_2$. The broken lines give classical limits for B(E2). Shown also are the experimental data for ^{129}La ($\gamma = 22^o$) and ^{131}La ($\gamma = 23^o$). The transition probabilities are given in terms of $\frac{5}{16\pi} Q_0^2$ where Q_0 is given by

$$Q_0 = \frac{3}{\sqrt{5\pi}} (1.2)^2 Z\beta A^{2/3} (\text{fm})^2 .$$

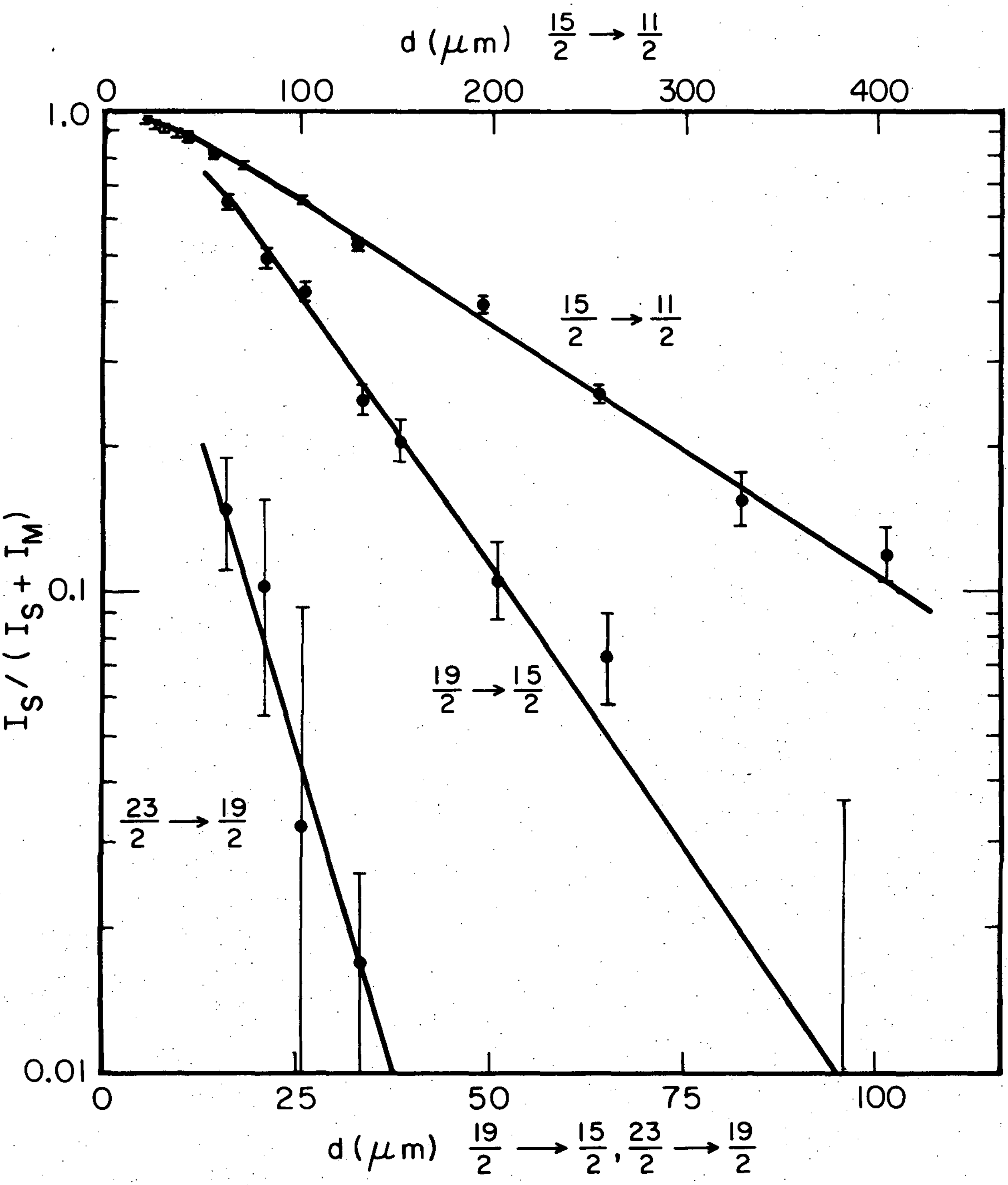

XBL753-2430

Fig. 1

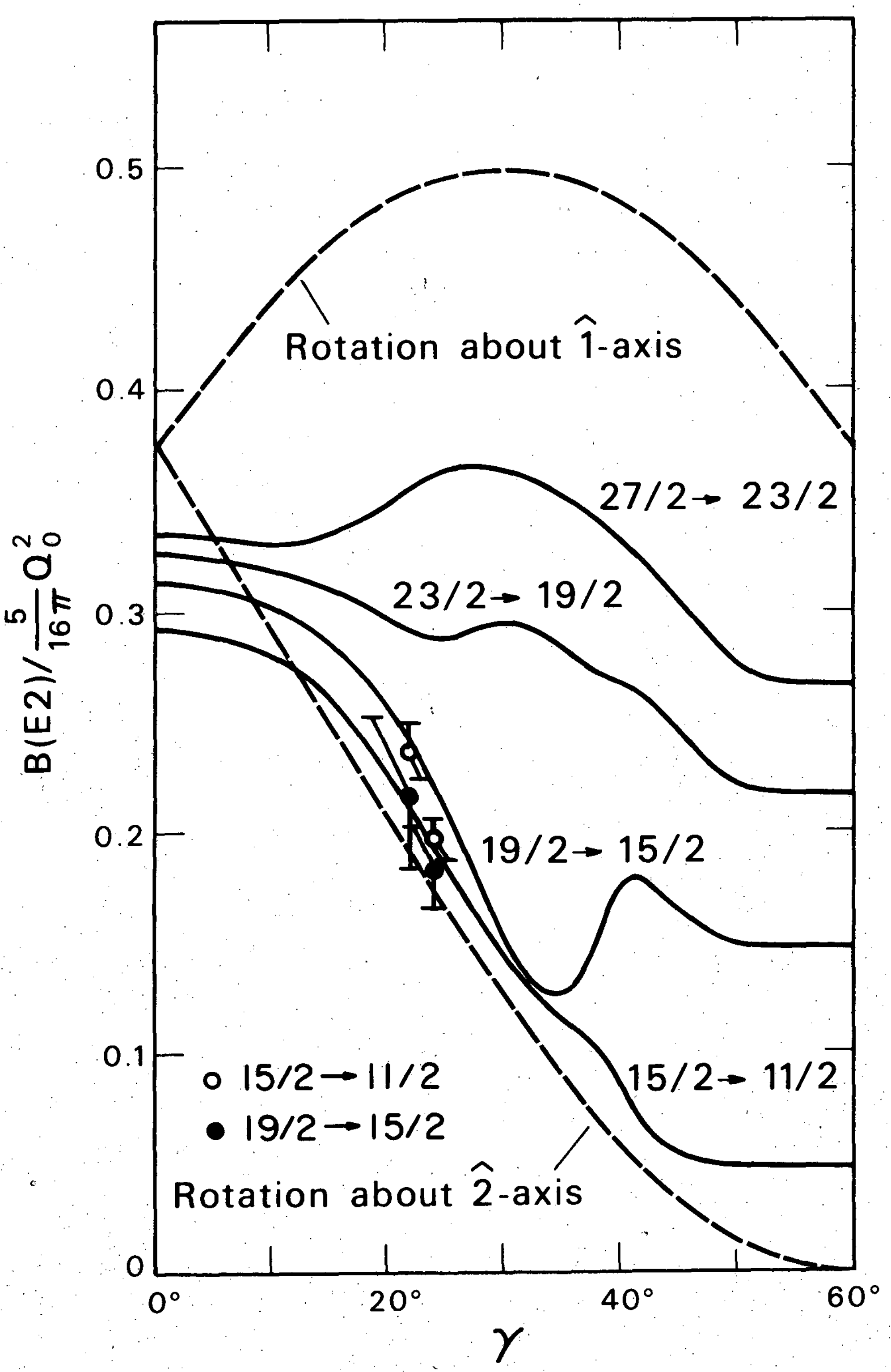

XBL 751-4616

Fig. 2

TECHNICAL INFORMATION DIVISION
LAWRENCE BERKELEY LABORATORY
UNIVERSITY OF CALIFORNIA
BERKELEY, CALIFORNIA 94720